

# SEMI-SUPERVISED UNDERWATER OBJECT DETECTION WITH IMAGE ENHANCEMENT GUIDED BY ATTRIBUTE-BASED DATA DISTRIBUTION

**Anonymous authors**

Paper under double-blind review

## ABSTRACT

Semi-supervised underwater object detection aims to improve the performance of detectors on unlabeled underwater images by leveraging knowledge from labeled ones. However, existing methods often overlook the distribution differences between labeled and unlabeled underwater images. In this paper, we propose a novel underwater image enhancement method guided by attribute-based data distribution (UIEG+), which focuses on reducing the discrepancies between enhanced and original unlabeled images across different attributes, thereby effectively addressing the challenges in semi-supervised underwater object detection. Specifically, we explore an underwater image enhancement strategy based on two attributes: color and scale distributions. For the color attribute, we construct a 3-dimensional grid memory, where each grid cell represents a color subspace and records the number of samples in that subspace. Similarly, for the scale attribute, we design a 1-dimensional vector memory that dynamically stores the number of samples in each scale subspace. Subsequently, we propose an effective sampling method to derive parameters for color and scale transformations based on the aforementioned distribution analysis, increasing the likelihood of transformations in low-distribution regions. To evaluate its effectiveness and superiority, massive semi-supervised underwater object detection experiments in multiple datasets have been conducted by integrating UIEG+ into existing semi-supervised object detection frameworks. The code will be released.

## 1 INTRODUCTION

With the development of deep learning, object detection models have also experienced unprecedented growth, and many outstanding detection models have been proposed (Ren et al., 2017; Tian et al., 2019; Carion et al., 2020). However, when dealing with underwater scenes and objects, these detectors still face challenges related to complexity and diversity. To address these issues, a simple solution is to gather a more extensive dataset that encompasses a wide range of scenes and object styles. Nevertheless, this is an extremely challenging task that requires significant resources and makes it difficult to cover all possible scenarios.

In recent years, semi-supervised object detection based on image enhancement has also emerged as a pivotal solution, which primarily emphasizes the generation of high-quality enhanced images accompanied by labels or pseudo-labels. Existing image enhancement methodologies for semi-supervised underwater object detection (SSUOD) can be broadly classified into two categories. The former encompasses traditional image enhancement techniques (Zhang et al., 2022; Peng et al., 2018; Liu et al., 2023b), which employ physics-based operations to manipulate various attributes such as color, scale, and contrast, often through random transformations, as illustrated in Fig. 1 (a). Despite their widespread application in semi-supervised object detection frameworks, such as the teacher-student model with weak and strong augmentations (Zhang et al., 2023b), these methods exhibit certain limitations: firstly, they fail to account for the distribution of unlabeled images across different attribute spaces, potentially resulting in the generation of unrealistic enhanced images that could detrimentally affect model training; secondly, they overlook the adverse effects of the imbalanced distribution of unlabeled images within these attribute spaces. The latter involves the construction of learnable networks (Jiang et al., 2022; Cong et al., 2023; Zhang et al., 2024) to

054  
055  
056  
057  
058  
059  
060  
061  
062  
063  
064  
065  
066  
067  
068  
069  
070  
071  
072  
073  
074  
075  
076  
077  
078  
079  
080  
081  
082  
083  
084  
085  
086  
087  
088  
089  
090  
091  
092  
093  
094  
095  
096  
097  
098  
099  
100  
101  
102  
103  
104  
105  
106  
107

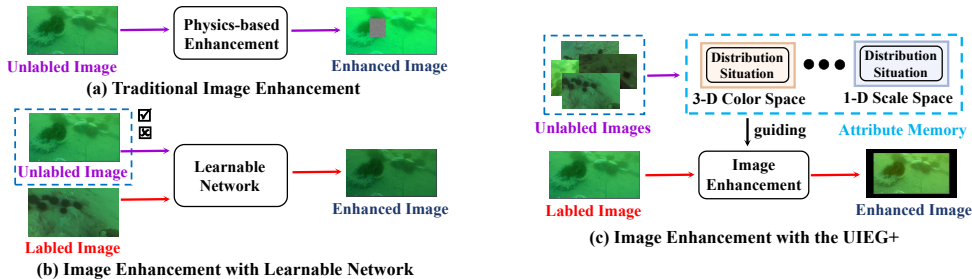


Figure 1: Comparison between the proposed UIEG+ and other methods. (a) Traditional image enhancement; (b) Image enhancement with learnable network; (c) Our UIEG+ method. The check mark and cross in the rectangular boxes indicate whether the unlabeled image is used or not.

achieve style transfer between labeled and unlabeled images. The works (Peng et al., 2023; Zhang et al., 2024) focus on designing end-to-end networks that directly facilitate style transfer across different domains. In contrast, other studies (Deng et al., 2022; Wang et al., 2023b) extract style information and utilize it to guide the content image through style transformation. However, these approaches also present limitations when applied to semi-supervised underwater detection: firstly, they are constrained to enhancing images within the three-dimensional color space, neglecting potential transformations in other attribute spaces, such as scale space; secondly, these methods are similarly challenged by the issue of imbalanced distribution previously mentioned.

**Contribution** Different from the aforementioned methodologies, this paper considers the actual distribution of unlabeled underwater images, which aims to mitigate the distributional discrepancies between enhanced and unlabeled underwater images. To be specific, we address the distribution of unlabeled underwater images in terms of color and scale attributes. For the color attribute, we develop a three-dimensional color memory, wherein each cell represents a three-dimensional color subspace within a defined range and records the number of unlabeled images in that subspace. Analogously, for the scale attribute, we construct a one-dimensional memory that records the number of unlabeled images in each cell. The color and scale subspaces of the images are determined using the mean values of each color channel and the average scale of all objects within the image. Subsequently, based on these distributional insights, we propose a sampling strategy to derive color and scale transformation parameters, thereby guiding image enhancement. This sampling method effectively balances enhanced images across different subspaces of color and scale. Ultimately, we integrate the proposed UIEG+ into existing SSOD frameworks to address semi-supervised underwater object detection, as shown in Fig. 1.

In summary, our contributions can be outlined as follows:

- We propose a novel underwater image enhancement method guided by attribute-based data distribution (UIEG+), which aims to reduce distributional differences between enhanced and unlabeled underwater images by analyzing the distribution of unlabeled images in terms of color and scale attributes.
- We incorporate the proposed UIEG+ into existing SSOD frameworks, thereby effectively addressing the challenges of semi-supervised underwater object detection.
- Our method achieves state-of-the-art performance on multiple semi-supervised underwater detection (SSUD) datasets and demonstrates significant improvements across various SSOD methods.

## 2 RELATED WORK

### 2.1 OBJECT DETECTION

Deep learning detectors have made significant advancements over the past few years. Currently, existing detection models are generally classified into two categories, i.e one- and two-stage detectors. One-stage detectors (e.g.FCOS (Tian et al., 2019), Yolo (Redmon & Farhadi, 2018), and

108 DETR (Carion et al., 2020)) directly predict the classes and rectangular boxes of objects on fea-  
109 ture maps without medium proposals. Different from one-stage detectors, two-stage detectors (Ren  
110 et al., 2017; Cai & Vasconcelos, 2018) design the region proposal network (RPN) to obtain more  
111 accurate proposals and further conduct the classification and regression of these proposals. In this  
112 work, we explain the principles of our method based on the PseCo framework (Li et al., 2022) with  
113 Faster-RCNN (Ren et al., 2017) detector and demonstrate its effectiveness and generalizability when  
114 applied to different detectors (Tian et al., 2019) in our experiments.

## 115 2.2 SEMI-SUPERVISED DETECTION

116  
117 Semi-supervised detection seeks to improve the performance of detectors on unlabeled images by  
118 exploring the training strategies on labeled and unlabeled images. One branch (Zhou et al., 2022;  
119 Liu et al., 2023a; Shehzadi et al., 2024) performs self-training on labeled and unlabeled images. The  
120 core idea is to acquire high-quality pseudo-labels or samples. Some works (Wang et al., 2021; Li  
121 et al., 2023) pay attention to uncertain regions or class imbalance problems. Despite their effective-  
122 ness, these methods are limited by the noise in predicted pseudo-labels or samples, which primarily  
123 arises from differences between labeled and unlabeled images and the selection of hyperparameters.  
124 Moreover, another popular trend (Jeong et al., 2019; Li et al., 2022; Wang et al., 2023a) is to employ  
125 consistency analysis of internal features or external predictions from the detection network to learn  
126 more robust feature representations or outputs. However, achieving more effective consistency guid-  
127 ance is challenging, particularly when it comes to the feature representation of foreground objects  
128 affected by various disturbances. In this work, we utilize our UIEG+ method instead of the strong  
129 augmentation found in previous teacher-student frameworks (Zhou et al., 2022; Li et al., 2022; Liu  
130 et al., 2023a), resulting in enhanced images that match the data distribution of the unlabeled images.

## 131 2.3 SEMI-SUPERVISED UNDERWATER DETECTION

132  
133 Semi-supervised underwater detection aims at improving the adaptation of detectors to various un-  
134 derwater scenes by leveraging both labeled and unlabeled images in the training process. Exist-  
135 ing works (Sharma et al., 2024; Noman et al., 2021) mainly address this issue by using current  
136 semi-supervised detection strategies. Different from these works, we propose an underwater image  
137 enhancement guided by attribute-based data distribution to reduce the distribution discrepancies be-  
138 tween enhanced images and the original unlabeled images in different attributes, effectively handling  
139 semi-supervised underwater object detection.

## 140 2.4 IMAGE ENHANCEMENT

141  
142 Image enhancement is an effective method to handle semi-supervised underwater detection. The  
143 previous works can be grouped into traditional underwater image enhancement (Zhang et al., 2022;  
144 Peng et al., 2018; Liu et al., 2023b) and learning-based underwater image enhancement (Jiang et al.,  
145 2022; Cong et al., 2023; Zhang et al., 2024). Traditional underwater image enhancement relies on  
146 physics-based operations that are manually defined for different attributes, *i.e.* color (Ancuti et al.,  
147 2012; Wang et al., 2018), contrast (Zhang et al., 2022), and scale. These works use random sampling  
148 to enhance images but do not account for the distribution of unlabeled images across different at-  
149 tributes in semi-supervised underwater detection. As a result, some unreasonable enhanced images  
150 can negatively impact the model’s training. In contrast, learning-based underwater image enhance-  
151 ment achieves the style transfer between different domain images by constructing the learnable  
152 network. While this approach can reduce style differences between enhanced and unlabeled images,  
153 it fails to address issues related to imbalanced style distribution in the unlabeled underwater images  
154 and differences in the distribution of other attributes (e.g., scale).

## 155 2.5 DIFFERENCES FROM OTHER WORKS

156  
157 In this work, we propose an underwater image enhancement method guided by attribute-based data  
158 distribution and integrate it into existing semi-supervised detection frameworks. Compared to the  
159 above image enhancement methods, our approach has the following differences. **First**, we consider  
160 the distribution of unlabeled underwater images in terms of color and scale attributes, and mitigate  
161 the impact of imbalanced distributions on enhanced images through a distribution-based sampling

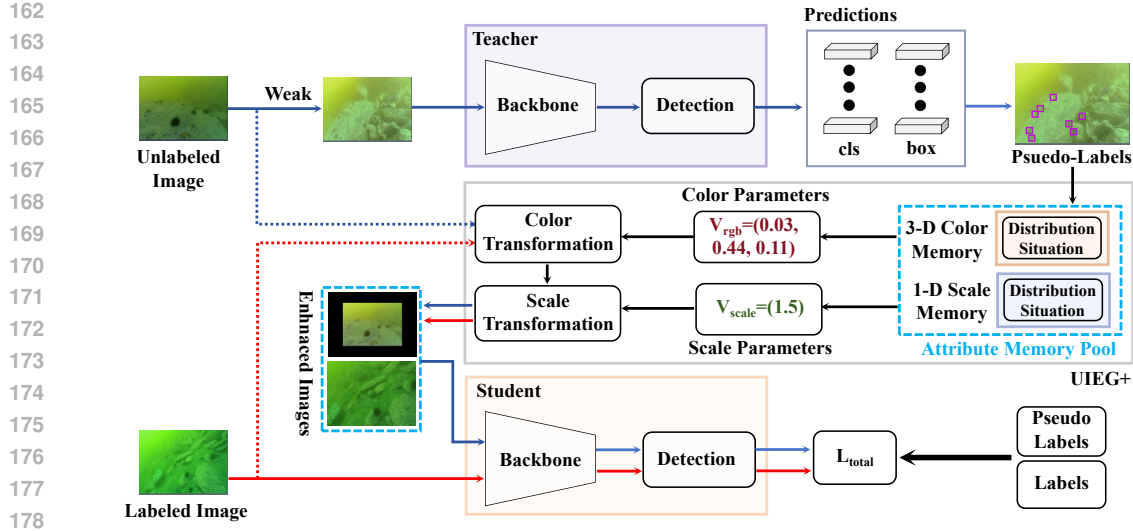


Figure 2: The framework of UIEG+-based semi-supervised underwater object detection, which is built upon the PseCo (Li et al., 2022) with Faster-RCNN (Ren et al., 2017) detector. Compared to the original PseCo, we replace the strong augmentation with our UIEG+ method.

method. **Second**, our method effectively enhances both labeled and unlabeled images without requiring additional training. In summary, our UIEG+ is a simple yet effective approach that boosts the performance of existing semi-supervised detection frameworks for underwater detection.

### 3 METHODOLOGY

#### 3.1 OVERALL SSUOD FRAMEWORK

Fig. 2 illustrates the framework of semi-supervised underwater object detection with UIEG+, which is constructed based on the PseCo (Li et al., 2022) with Faster-RCNN (Ren et al., 2017) detector and the proposed UIEG+. Given the labeled image  $(x_l, y_l)$  and the unlabeled image  $x_u$ , we first perform weak augmentation on the unlabeled underwater image and generate its pseudo-labels  $\hat{y}_u$  using the teacher detector. Then, we update the 3-D color and 1-D scale memories with the unlabeled underwater image and its pseudo-labels. Following this, we sample transformation parameters for color and scale from these memories and apply them to both labeled and unlabeled underwater images, producing enhanced images with corresponding labels and pseudo-labels, i.e.,  $(x_l^{ie}, y_l^{ie})$  and  $(x_u^{ie}, \hat{y}_u^{ie})$ . Finally, the student detector is trained using these labeled, unlabeled and enhanced images. Therefore, the unified optimization loss is mathematically described as follows:

$$\begin{aligned} \mathcal{L}_{\text{total}} = & \mathcal{L}_{\text{det}}(x_l, y_l) + \gamma_l^{ie} \mathcal{L}_{\text{det}}(x_l^{ie}, y_l^{ie}) \\ & + \gamma_u^{ie} \mathcal{L}_{\text{det}}(x_u^{ie}, \hat{y}_u^{ie}) \end{aligned} \quad (1)$$

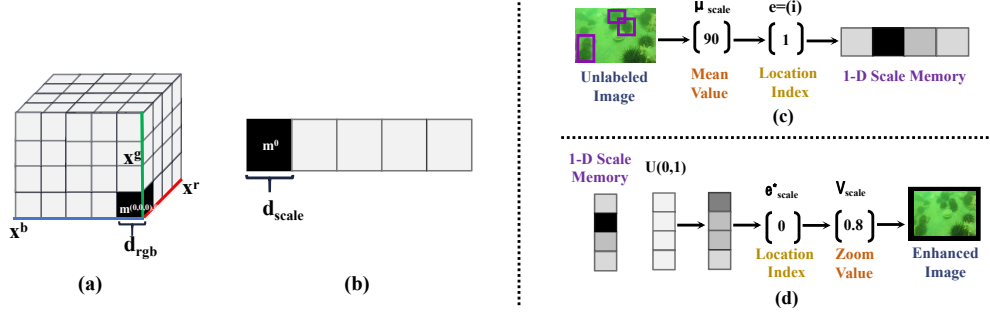
where  $\gamma_l^{ie}$  and  $\gamma_u^{ie}$  are weight coefficients used to balance three loss terms, and  $\mathcal{L}_{\text{det}}$  denotes the detection loss of the base student detector Faster-RCNN (Ren et al., 2017).

Notably, our UIEG+ can be applied to various semi-supervised object detection frameworks (e.g., DenseTeacher (Zhou et al., 2022) and ARSL (Liu et al., 2023a)). In this work, we take PseCo (Li et al., 2022) with Faster-RCNN as an example to illustrate the principles of UIEG+ and explain how to integrate it into PseCo. In addition, we demonstrate the generality of our UIEG+ by applying it to various SSOD frameworks in the experiments.

#### 3.2 UNDERWATER IMAGE ENHANCEMENT GUIDED BY ATTRIBUTE-BASED DATA DISTRIBUTION

In this section, we propose an underwater image enhancement method guided by attribute-based data distribution to minimize the distribution differences between enhanced and unlabeled underwater

216  
217  
218  
219  
220  
221  
222  
223  
224  
225  
226



227 Figure 3: (a) 3-D color memory; (b) 1-D scale memory; (c) The Process of storing scale information;  
228 (d) The process of image enhancement in scale space.

229  
230  
231  
232  
233  
234  
235  
236

images. This approach effectively improves the relevance and diversity of the enhanced images. As shown in Fig. 2, to end this, we first create an attribute memory pool consisting of the 3-D color memory and 1-D scale memory. Subsequently, we analyze unlabeled images with pseudo-labels in color and scale spaces separately, updating the corresponding memory cells by assigning them to different subspaces. Following this, we proceed to enhance the images based on the distribution of the unlabeled images within these memory pools.

237  
238  
239  
240  
241  
242  
243  
244  
245

**Color and Scale Memories** Color and scale memories are used to record the number of unlabeled underwater images in different subspaces. Specifically, we divide the 3-dimensional color space, with each dimension ranging from 0 to 1, into  $(\lfloor 1/d_{rgb} \rfloor + 1)^3$  subspaces using the interval step  $d_{rgb}$  in each dimension. Here,  $\lfloor \cdot \rfloor$  is the floor operation, and  $(\lfloor 1/d_{rgb} \rfloor + 1)$  is labeled as  $N_{rgb}$ . Following this, we construct a 3-D color memory  $M_{rgb} \in \mathbb{R}^{N_{rgb} \times N_{rgb} \times N_{rgb}}$ , where each cell corresponds to a subspace with the size of  $d_{rgb} \times d_{rgb} \times d_{rgb}$ . Similarly, we divide the scale space, ranging from 0 to  $\infty$ , into  $\lfloor 1/d_{scale} \rfloor + 1$  subspaces using the interval step  $d_{scale}$ . Meanwhile, the scale memory is constructed, where each cell corresponds to a subspace with the size of  $d_{scale}$ . The structure of color and scale memories is shown in Fig. 3 (a) and (b).

246  
247  
248  
249

**Sample Distribution** Following the establishment of the color and scale memories, we analyze the distribution of unlabeled underwater images. Given unlabeled image  $x_u \in \mathbb{R}^{3 \times H \times W}$ , we normalize it to the range of  $[0, 1]$  and then compute the mean value of  $x_u$  for each dimension, denoted as  $u_{rgb} \in \mathbb{R}^3$ .

250  
251  
252

$$u_{rgb}^k = \frac{1}{HW} \sum_{i,j} x_u^{k,i,j} \quad (2)$$

253  
254  
255  
256

where  $H$  and  $W$  are the height and width of the unlabeled underwater image.  $k$  is the number of dimensions of the image. Then, we further allocate the image  $x_u$  into the color memory space using  $u_{rgb} \in \mathbb{R}^3$  to determine the corresponding position index  $e_{rgb} \in \mathbb{Z}^3$ . By utilizing the index  $e_{rgb}$ , the color memory  $M_{rgb}$  is updated as follows.

257

$$e_{rgb}^k = \lfloor u_{rgb}^k / d_{rgb} \rfloor \quad (3)$$

258

$$M_{rgb}(e_{rgb}) = M_{rgb}(e_{rgb}) + 1 \quad (4)$$

259  
260

Similarly, the scale memory is updated by determining the location index of the unlabeled underwater image in it, which can be formulated as:

261  
262  
263  
264  
265

$$u_{scale} = \frac{1}{N_{box}} \sum_i \sqrt{(B_{i,2} - B_{i,0}) \cdot (B_{i,3} - B_{i,1})} \quad (5)$$

266

$$M_{scale}(e_{scale}) = M_{scale}(e_{scale}) + 1, \quad e_{scale} = \lfloor u_{scale} / d_{scale} \rfloor \quad (6)$$

267  
268  
269

where  $B \in \mathbb{R}^{N_{box} \times 4}$  represents the bounding boxes of all objects in the unlabeled underwater image, obtained by the teacher detector. The process of analyzing the distribution of unlabeled underwater images in the scale space is illustrated in Fig 3 (c).

**Image Enhancement** To reduce the distribution differences between enhanced and unlabeled images, in this section, we explore the image enhancement method based on the distributions of unlabeled underwater images in color and scale space. In detail, we first perform the color transformation for input images. As shown in Fig. 2, we utilize the distribution information in the color memory to determine the sampling probability of each cell within it, which can be formulated as

$$P_{rgb} = \left(1 - \frac{M_{rgb}}{\max(M_{rgb})}\right) \cdot U_{3d} \cdot I_{rgb} \quad (7)$$

$$I_{rgb} = \begin{cases} 1.0, & M_{rgb} > 0 \\ 0.0, & \text{otherwise} \end{cases} \quad (8)$$

where  $U_{3d}$  is a 3-dimensional matrix obtained by randomly sampling from a uniform distribution in the range  $[0, 1]$ , which has the same size as  $M$ . The color transformation parameter is then determined based on the sampling probability, which can be formulated as

$$e_{rgb}^* = \operatorname{argmax}(P_{rgb}) \quad (9)$$

$$V_{rgb} = (e_{rgb}^* + \sigma_{rgb}) \cdot d_{rgb} \quad (10)$$

where  $\sigma_{rgb}$  is a contrast bias less than 1.  $\operatorname{argmax}(\cdot)$  is the function that finds the index of the maximum value.  $V_{rgb}$  is the final parameter of the color transformation. By employing the parameter  $V_{rgb}$ , we perform the color transformation for input images, which can be formulated as

$$x^{ie} = x + \eta_{rgb} \cdot (V_{rgb} - u_{rgb}^x) \quad (11)$$

where  $\eta_{rgb}$  is a constant and  $u_{rgb}^x$  is the mean value of  $x$  in each dimension. Following this, we further derive the scale transformation parameter using a process similar to that used for the color transformation, which can be formulated as

$$P_{scale} = \left(1 - \frac{M_{scale}}{\max(M_{scale})}\right) \cdot U_{1d} \cdot I_{scale}, \quad I_{scale} = \begin{cases} 1.0, & M_{scale} > 0 \\ 0.0, & \text{otherwise} \end{cases} \quad (12)$$

$$V_{scale} = \frac{(e_{scale}^* + \sigma_{scale}) \cdot d_{scale}}{u_{scale}^x}, \quad e_{scale}^* = \operatorname{argmax}(P_{scale}) \quad (13)$$

where  $U_{1d}$  is a 1-dimensional matrix and  $\sigma_{scale}$  is a contrast bias less than 1.  $u_{scale}^x$  is the mean scale value of all objects in the image  $x$ .  $V_{scale}$  is the scale rate of the image  $x$ . By applying  $V_{scale}$  to the interpolate operation (Jaderberg et al., 2015), we achieve the scale transformation of  $x$ . Fig. 3 (d) shows the process of enhancing the image in terms of scale.

Finally, in this work, we enhance the images of both unlabeled and labeled datasets using the proposed UIEG+ to increase the rationality and diversity of the enhanced images, effectively addressing the problem of semi-supervised underwater object detection with Eq. 1.

### 3.3 OPTIMIZATION

The training process of our UIEG+-based SSU detection framework is meticulously structured into two distinct stages to ensure optimal performance. In Stage 1, we concentrate exclusively on training the teacher detector using only the labeled images. In Stage 2, we focus on optimizing the student detector training on both labeled and unlabeled images. The objective here is to leverage the vast amount of unlabeled data to enhance the model’s generalization capabilities. With the loss function in Eq. 1 to guide the learning process of the student detector, we can continuously update the teacher detector using the exponential moving average (EMA) strategy to ensure that it evolves alongside the student detector, which can be expressed as:

$$\theta_t = \delta \cdot \theta_t + (1 - \delta) \cdot \theta_s \quad (14)$$

where  $\theta_t$  and  $\theta_s$  indicate the parameters of the teacher and student detectors.  $\delta$  represents the EMA rate.

Table 1: Results of our approach and comparison to state-of-the-arts on DUO. The best two results are shown in red and blue fonts, respectively.

Method	Detector	Holothurian	Echinus	Scallop	Starfish	$mAP_{50}$	mAP
Labeled Only	FCOS	66.8	86.5	21.0	83.6	64.5	39.2
DenseTeacher (Zhou et al., 2022)	FCOS	77.7	88.7	35.2	87.9	72.4	48.9
ARSL (Liu et al., 2023a)	FCOS	78.1	85.2	42.9	88.5	73.7	35.4
Unbiased-Teacher2 (Liu et al., 2022)	FCOS	82.4	86.8	50.7	88.8	77.2	56.8
Consistent-Teacher (Wang et al., 2023a)	FRCNN	84.1	87.6	<b>52.3</b>	86.8	77.7	<b>60.0</b>
Labeled Only	FRCNN	66.1	85.6	16.8	84.3	63.2	40.4
Soft Teacher (Xu et al., 2021)	FRCNN	84.9	88.2	44.3	89.2	76.6	53.9
PseCo (Li et al., 2022)	FRCNN	<b>85.7</b>	88.5	48.7	89.3	<b>78.0</b>	56.8
MixTeacher (Liu et al., 2023c)	FRCNN	85.4	<b>88.9</b>	46.6	<b>89.6</b>	77.6	56.3
Ours (DenseTeacher)	FCOS	79.1	88.4	41.1	87.3	74.0	50.9
Ours (ARSL)	FCOS	78.8	85.5	45.4	88.5	74.6	36.1
Ours (PseCo)	FRCNN	<b>85.9</b>	<b>89.4</b>	<b>54.3</b>	<b>90.3</b>	<b>80.0</b>	<b>57.2</b>
oracle	FCOS	80.9	89.3	40.7	88.1	74.8	53.6
oracle	FRCNN	87.0	90.7	61.9	91.3	82.7	62.6

## 4 EXPERIMENTS

### 4.1 IMPLEMENTATION

Our framework is implemented based on the PseCo framework (Li et al., 2022) in PyTorch (Paszke et al., 2019). Similarly, we use Faster-RCNN (Ren et al., 2017) with ResNet-50 (He et al., 2016) pre-trained on ImageNet (Krizhevsky et al., 2012) as teacher and student detectors. The model is trained with a learning rate of  $1e-3$ , momentum of 0.9, and weight decay of  $1e-4$ .  $\gamma_l^{ie}$  and  $\gamma_u^{ie}$  are set to 1.0 and 0.1 in Eq. 1, respectively.  $d_{rgb}$  and  $d_{scale}$  are set to 0.05 and 64, respectively.  $\eta_{rgb}$  is 0.3 in Eq. 11. To evaluate the effectiveness and generalizability of our UIEG+, we integrate it into two additional SSOD frameworks, *i.e.* ARSL (Liu et al., 2023a) and DenseTeacher (Zhou et al., 2022), utilizing both FCOS (Tian et al., 2019) as the base detectors. Specifically, in both ARSL and DenseTeacher, we substitute only the strong augmentation with our UIEG+, keeping all other components unchanged.

### 4.2 DATASETS

In this work, we conducted experiments on two underwater datasets to verify the effectiveness and superiority of the proposed UIEG+. For all experiments, we take the standard mean average precision (mAP) at different IoU thresholds (*e.g.*,  $AP_{50:95}$  denoted as mAP,  $AP_{50}$ ) as our evaluation metrics.

- **DUO** The DUO (Liu et al., 2021) dataset has 6671 images for training and 1111 images for evaluation with shared four classes, *i.e.* Holothurian, Echinus, Scallop, and Starfish. Following works (Li et al., 2022; Hua et al., 2023), we randomly sample 10% of the training images as labeled data, while the remaining images are used as unlabeled data. The testing images are used for evaluation.
- **URPC** The URPC dataset, collected from the Underwater Robot Picking Contest, includes 16247 training images and 4062 testing images, with four classes *i.e.* Holothurian, Echinus, Scallop, and Starfish. Similarly, we randomly sample 10% of the training images as labeled data, leaving the remaining images as unlabeled data. Additionally, the testing images are used for evaluation.

### 4.3 RESULT ANALYSIS

In this section, we present the evaluation results of current state-of-the-art SSOD methods and demonstrate the effectiveness of our UIEG+ by applying it to other SSOD frameworks on three sets of experiments built on two underwater datasets, *e.g.* DUO and URPC. The “Labeled Only”

Table 2: Results of our approach and comparison to state-of-the-arts on URPC. The best two results are shown in red and blue fonts, respectively.

Method	Detector	Holothurian	Echinus	Scallop	Starfish	$AP_{50}$	mAP
Labeled Only	FCOS	64.6	74.1	66.8	70.2	68.9	30.2
DenseTeacher (Zhou et al., 2022)	FCOS	74.5	89.6	73.2	81.3	79.7	41.9
ARSL (Liu et al., 2023a)	FCOS	75.0	88.0	73.8	80.8	79.4	34.3
Unbiased-Teacher <sub>v2</sub> (Liu et al., 2022)	FCOS	70.8	80.6	63.9	75.7	72.8	38.9
Consistent-Teacher (Wang et al., 2023a)	FCOS	79.2	84.2	72.3	78.9	78.7	43.3
Labeled Only	FRCNN	69.5	87.6	70.9	79.5	76.9	39.3
Soft Teacher (Xu et al., 2021)	FRCNN	78.3	88.2	72.3	79.4	79.5	43.2
PseCo (Li et al., 2022)	FRCNN	80.6	87.3	74.7	79.9	80.6	44.3
MixTeacher (Liu et al., 2023c)	FRCNN	79.5	87.9	73.9	79.1	80.1	43.8
Ours (DenseTeacher)	FCOS	77.4	89.5	74.8	82.4	81.0	43.9
Ours (ARSL)	FCOS	76.3	88.7	74.3	81.3	80.2	34.7
Ours (PseCo)	FRCNN	80.6	89.8	76.2	81.8	82.1	44.8
oracle	FCOS	86.2	92.3	80.5	86.4	86.3	50.0
oracle	FRCNN	88.0	92.6	82.3	86.6	87.4	51.7

Table 3: Results of our approach and comparison to state-of-the-arts on DUO and URPC. The best two results are shown in red and blue fonts, respectively.

Method	Detector	Holothurian	Echinus	Scallop	Starfish	$AP_{50}$	mAP
Unbiased-Teacher <sub>v2</sub> (Liu et al., 2022)	FCOS	62.8	78.2	48.0	74.2	65.8	33.4
ARSL (Liu et al., 2023a)	FCOS	66.0	83.2	56.6	80.1	71.5	29.8
PseCo (Li et al., 2022)	FRCNN	72.5	85.0	51.1	79.6	72.0	35.0
MixTeacher (Liu et al., 2023c)	FRCNN	68.4	85.2	47.0	79.8	70.1	34.2
Ours (ARSL)	FCOS	66.6	84.6	63.5	79.3	73.5	30.5
Ours (PseCo)	FRCNN	71.5	83.7	63.9	73.7	73.2	35.5

results indicate that the model is trained only on labeled images and then evaluated on testing images. The “oracle” results indicate the model is trained on all training images (including labeled and unlabeled images) and evaluated on testing images.

**DUO** Tab. 1 exhibits the evaluation results on DUO dataset. As shown in Tab. 1, when the proposed UIEG+ is applied to DenseTeacher, ARSL, and PseCo, our approach improves  $AP_{50}$  from 72.4%, 73.7% and 78.0% to 74.0%, 74.6% and 80.0%, resulting in gains of 1.6%, 0.9% and 2.0%. Additionally, our method achieves mAP improvements of 2.0%, 0.7% and 0.4%, respectively. Compared to the baseline (Labeled only) on Faster R-CNN and FCOS detectors, our UIEG+ demonstrates a significant improvement, further proving the effectiveness of our approach.

**URPC** We display the comparison results on URPC in Tab. 2. As shown in Tab. 2, when strong augmentation in DenseTeacher, ARSL and PseCo is replaced by our UIEG+, they obtain  $AP_{50}$  scores of 81.0%, 80.2%, and 82.1%, respectively, achieving clear improvement with 1.3%, 0.8% and 1.5% gains. Meanwhile, our method also acquire mAP gains of 2.0%, 0.4% and 0.5% over DenseTeacher, ARSL, and PseCo, respectively. Additionally, compared to the baseline (Labeled Only), we achieve  $AP_{50}$  gains of 12.1% (81.0% vs. 68.9%) on the FCOS detector, and  $AP_{50}$  gains of 5.2% (82.1% vs. 76.9%) on the Faster R-CNN detector, showing the effectiveness of our UIEG+.

**DUO-to-URPC** To further evaluate our UIEG+ method, we report the comparison results on DUO and URPC in Tab. 3. In this experiment, we use 10% of the training images from DUO as labeled data and 90% of the training images from URPC as unlabeled data. Additionally, the testing images from URPC are utilized for evaluation. As shown in Tab. 3, when our UIEG+ is employed to SSOD frameworks of ARSL and PseCo, these frameworks obtain  $AP_{50}$  gains of 2.0% (71.5% vs 73.5%) and 1.2% (72.0% vs 73.2%), respectively. Moreover, our method also acquire mAP gains of 0.7%, and 0.5% on ARSL and PseCo, verifying the effectiveness of our method.



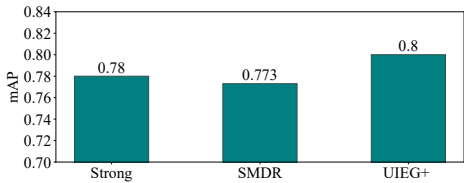


Figure 4: Comparison between image enhancement methods.

Table 4: Effectiveness of important components on URPC.

CTransform	STransform	AP <sub>50</sub>
		73.1
✓		77.6
✓	✓	80.0

#### 4.4 ABLATION STUDY

To study the effectiveness of different components and analyze important weights in our UIEG+, we conduct an ablation study based on PseCo framework on DUO dataset.

**Effectiveness of different components** To analyze the effectiveness of image transformations with different attributes (*e.g.*, color and scale) in our UIEG+, we report comparison results of our UIEG+ with various attributes, as shown in Tab. 4. Here, "CTransform" and "STransform" represent color and scale transformations, respectively. From Tab. 4, we find that UIEG+ with color transformation significantly improves the performance of PseCo from 73.1% AP<sub>50</sub> to 77.6% AP<sub>50</sub>. When employing UIEG+ with all two transformations, we obtain the best AP<sub>50</sub> of 80.0%, evidencing the effectiveness of color and scale transformations in UIEG+.

**Comparison of sampling methods** As shown in Tab. 5, we compare the proposed distribution-based sampling and random sampling for color and scale transformation parameters in UIEG+. Random sampling omits the front part of  $U \cdot I$  in Eq. 7 and 12. From Tab. 5, we find that our distribution-based sampling achieves a significant gain of 1.3% compared to random sampling, demonstrating the superiority of our approach.

Table 5: Comparison of different sampling methods of transformation parameters.

	Random	Ours
mAP	78.7	80.0

**Comparison of image enhancement methods** To verify the superiority of our UIEG+ than other image enhancement methods, *e.g.*, randomly strong augmentation and SMDR (Zhang et al., 2023a) that is an image enhancement network, we show comparison results in Fig. 4. From Fig. 4, we observe that our UIEG+ achieves AP<sub>50</sub> gains of 2.0% and about 2.3% compared to randomly applied strong augmentation and SMDR.

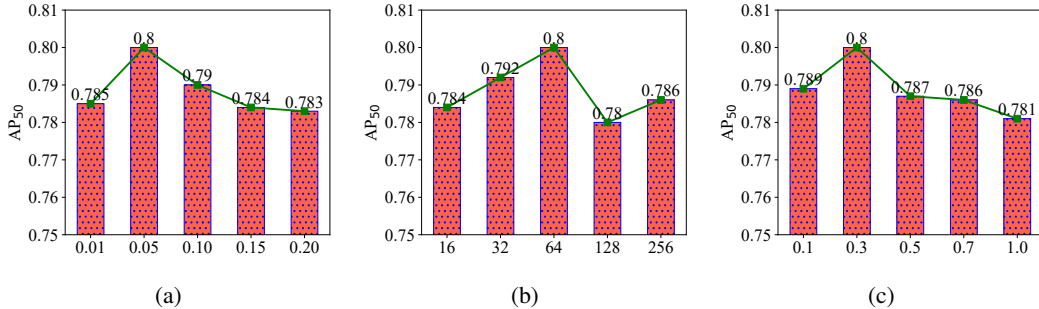
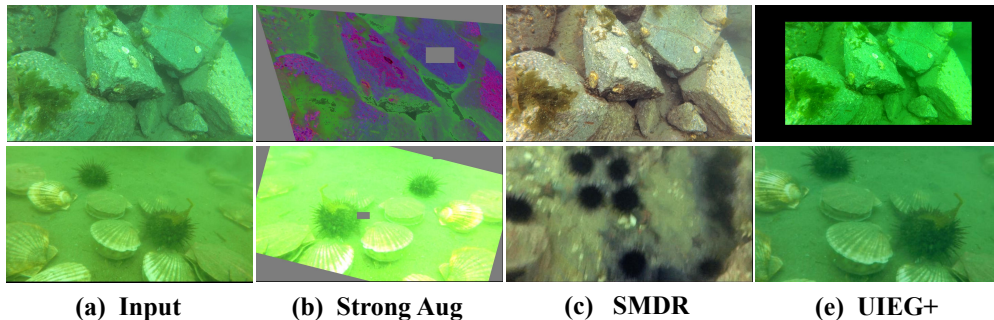


Figure 5: Weight analysis. (a) represents analysis results of  $d_{rgb}$ ; (b) represents analysis results of  $d_{scale}$ ; (c) represents analysis results of  $\eta_{rgb}$ .

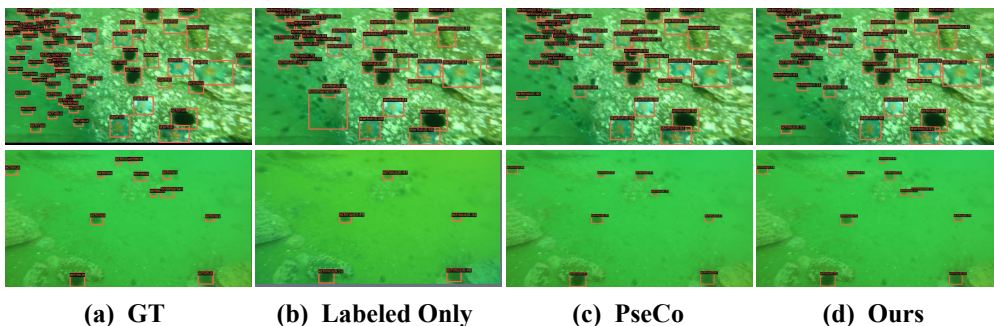
**Analysis on hyperparameter** To explore the effects of weights  $d_{rgb}$  in Eq. 3,  $d_{scale}$  in Eq. 6 and  $\eta_{rgb}$  in Eq. 11, we conduct ablations in Tab. 5a, 5b and 5c. As shown in Tab. 5a and 5b, both  $d_{rgb} = 0.05$  and  $d_{scale} = 64$  achieve the best AP<sub>50</sub> score of 80.0%, respectively. Larger and smaller values of  $d_{rgb}$  and  $d_{scale}$  can reduce the effectiveness of our UIEG+. In addition, from Tab. 5c, we observe that  $\eta_{rgb} = 0.3$  obtains the best AP<sub>50</sub> score.

486  
487  
488  
489  
490  
491  
492  
493  
494  
495  
496



497 Figure 6: Visual comparisons of our image enhancement method with other methods. The first row  
498 of images is from DUO, and the last row is from URPC.

499  
500  
501  
502  
503  
504  
505  
506  
507  
508  
509  
510



511 Figure 7: Visual results of PseCo trained with different underwater image enhancement methods  
512 on DUO and URPC. (a) shows the ground truth; (b) displays the visual results from the detector  
513 trained exclusively on labeled images; (c) presents the results obtained through the PseCo method;  
514 (d) illustrates the visual results using our UIEG+. The first row of images is from DUO, and the last  
515 row is from URPC.

516  
517

#### 518 4.5 VISUAL ANALYSIS

519  
520  
521

To provide a clearer understanding of the effectiveness of our image enhancement method and its effect on improving SSOD framework performance, we show some visualization samples in Fig. 6 and 7.

522  
523  
524  
525  
526  
527

**Visual comparisons of image enhancement methods** Fig. 6 shows visual comparisons of our image enhancement method with other methods (*e.g.*, strong augmentation and SMDR). From Fig. 6, we can see that strong augmentation can generate unrealistic enhanced images in contrast to the original unlabeled images, negatively impacting detector performance during training. However, our UIEG+ method produces more realistic enhanced images by aligning with the distribution of unlabeled underwater images in terms of color and scale attributes.

528  
529  
530  
531

**Visual detection results** Fig. 7 provide some visual results of PseCo trained using different image enhancement methods on DUO and URPC datasets. It demonstrates that our UIEG+ can significantly enhance the performance of PseCo for semi-supervised underwater object detection.

532  
533  
534

## 535 5 CONCLUSIONS

536  
537  
538  
539

In this paper, we propose a novel underwater image enhancement method guided by attribute-based data distribution (UIEG+) from a novel perspective, which reduces the differences in color and scale spaces between enhanced and unlabeled images. More importantly, UIEG+ can be flexibly integrated into various SSOD frameworks with different detectors, such as DenseTeacher, ARSL, PseCo, etc. Extensive experimental result can validate the effectiveness and generality of the proposed UIEG+ across multiple benchmarks.

## REFERENCES

- 540  
541  
542 Cosmin Ancuti, Codruta Orniana Ancuti, Tom Haber, and Philippe Bekaert. Enhancing underwa-  
543 ter images and videos by fusion. In *2012 IEEE Conference on Computer Vision and Pattern*  
544 *Recognition*, pp. 81–88, 2012.
- 545  
546 Zhaowei Cai and Nuno Vasconcelos. Cascade r-cnn: Delving into high quality object detection. In  
547 *2018 IEEE/CVF Conference on Computer Vision and Pattern Recognition*, pp. 6154–6162, 2018.
- 548  
549 Nicolas Carion, Francisco Massa, Gabriel Synnaeve, Nicolas Usunier, Alexander Kirillov, and  
550 Sergey Zagoruyko. End-to-end object detection with transformers. In Andrea Vedaldi, Horst  
551 Bischof, Thomas Brox, and Jan-Michael Frahm (eds.), *Computer Vision – ECCV 2020*, pp. 213–  
229, Cham, 2020. Springer International Publishing.
- 552  
553 Runmin Cong, Wenyu Yang, Wei Zhang, Chongyi Li, Chun-Le Guo, Qingming Huang, and Sam  
554 Kwong. Pugan: Physical model-guided underwater image enhancement using gan with dual-  
555 discriminators. *IEEE Transactions on Image Processing*, 32:4472–4485, 2023.
- 556  
557 Yingying Deng, Fan Tang, Weiming Dong, Chongyang Ma, Xingjia Pan, Lei Wang, and Changsheng  
558 Xu. Stytr<sup>2</sup>: Image style transfer with transformers. In *IEEE Conference on Computer Vision and*  
*Pattern Recognition (CVPR)*, 2022.
- 559  
560 Kaiming He, Xiangyu Zhang, Shaoqing Ren, and Jian Sun. Deep residual learning for image recog-  
561 nition. In *CVPR*, 2016.
- 562  
563 Wei Hua, Dingkan Liang, Jingyu Li, Xiaolong Liu, Zhikang Zou, Xiaoqing Ye, and Xiang Bai.  
564 Sood: Towards semi-supervised oriented object detection. In *2023 IEEE/CVF Conference on*  
*Computer Vision and Pattern Recognition (CVPR)*, pp. 15558–15567, 2023.
- 565  
566 Max Jaderberg, Karen Simonyan, Andrew Zisserman, and koray kavukcuoglu. Spatial transformer  
567 networks. In C. Cortes, N. Lawrence, D. Lee, M. Sugiyama, and R. Garnett (eds.), *Advances in*  
568 *Neural Information Processing Systems*, volume 28. Curran Associates, Inc., 2015.
- 569  
570 Jisoo Jeong, Seungeui Lee, Jeesoo Kim, and Nojun Kwak. Consistency-based semi-supervised  
571 learning for object detection. In *Advances in Neural Information Processing Systems*, volume 32,  
2019.
- 572  
573 Zhiying Jiang, Zhuoxiao Li, Shuzhou Yang, Xin Fan, and Risheng Liu. Target oriented perceptual  
574 adversarial fusion network for underwater image enhancement. *IEEE Transactions on Circuits*  
575 *and Systems for Video Technology*, 32(10):6584–6598, 2022.
- 576  
577 Alex Krizhevsky, Ilya Sutskever, and Geoffrey E Hinton. Imagenet classification with deep convo-  
lutional neural networks. *NIPS*, 2012.
- 578  
579 Gang Li, Xiang Li, Yujie Wang, Yichao Wu, Ding Liang, and Shanshan Zhang. Pseco: Pseudo  
580 labeling and consistency training for semi-supervised object detection. In Shai Avidan, Gabriel  
581 Brostow, Moustapha Cissé, Giovanni Maria Farinella, and Tal Hassner (eds.), *Computer Vision –*  
582 *ECCV 2022*, pp. 457–472, Cham, 2022. Springer Nature Switzerland.
- 583  
584 Jiaming Li, Xiangru Lin, Wei Zhang, Xiao Tan, Yingying Li, Junyu Han, Errui Ding, Jingdong  
585 Wang, and Guanbin Li. Gradient-based sampling for class imbalanced semi-supervised object  
586 detection. In *2023 IEEE/CVF International Conference on Computer Vision (ICCV)*, pp. 16344–  
16354, 2023.
- 587  
588 Chang Liu, Weiming Zhang, Xiangru Lin, Wei Zhang, Xiao Tan, Junyu Han, Xiaomao Li, Errui  
589 Ding, and Jingdong Wang. Ambiguity-resistant semi-supervised learning for dense object detec-  
590 tion. In *Proceedings of the IEEE/CVF Conference on Computer Vision and Pattern Recognition*  
591 *(CVPR)*, pp. 15579–15588, June 2023a.
- 592  
593 Chongwei Liu, Haojie Li, Shuchang Wang, Ming Zhu, Dong Wang, Xin Fan, and Zihui Wang. A  
dataset and benchmark of underwater object detection for robot picking. In *2021 IEEE Interna-  
tional Conference on Multimedia & Expo Workshops (ICMEW)*, pp. 1–6, 2021.

- 594 Liang Liu, Boshen Zhang, Jiangning Zhang, Wuhao Zhang, Zhenye Gan, Guanzhong Tian, Wenbing  
595 Zhu, Yabiao Wang, and Chengjie Wang. Mixteacher: Mining promising labels with mixed scale  
596 teacher for semi-supervised object detection. In *2023 IEEE/CVF Conference on Computer Vision  
597 and Pattern Recognition (CVPR)*, pp. 7370–7379, 2023b.
- 598  
599 Liang Liu, Boshen Zhang, Jiangning Zhang, Wuhao Zhang, Zhenye Gan, Guanzhong Tian, Wenbing  
600 Zhu, Yabiao Wang, and Chengjie Wang. Mixteacher: Mining promising labels with mixed scale  
601 teacher for semi-supervised object detection. In *2023 IEEE/CVF Conference on Computer Vision  
602 and Pattern Recognition (CVPR)*, pp. 7370–7379, 2023c.
- 603 Yen-Cheng Liu, Chih-Yao Ma, and Zsolt Kira. Unbiased teacher v2: Semi-supervised object de-  
604 tection for anchor-free and anchor-based detectors. In *2022 IEEE/CVF Conference on Computer  
605 Vision and Pattern Recognition (CVPR)*, pp. 9809–9818, 2022.
- 606 Md Kislun Noman, Syed Mohammed Shamsul Islam, Jumana Abu-Khalaf, and Paul Lavery. Multi-  
607 species seagrass detection using semi-supervised learning. In *2021 36th International Conference  
608 on Image and Vision Computing New Zealand (IVCNZ)*, pp. 1–6, 2021.
- 609 Adam Paszke, Sam Gross, Francisco Massa, Adam Lerer, James Bradbury, Gregory Chanan, Trevor  
610 Killeen, Zeming Lin, Natalia Gimelshein, Luca Antiga, et al. Pytorch: An imperative style, high-  
611 performance deep learning library. *NeurIPS*, 2019.
- 612 Lintao Peng, Chunli Zhu, and Liheng Bian. U-shape transformer for underwater image enhance-  
613 ment. *IEEE Transactions on Image Processing*, 32:3066–3079, 2023.
- 614 Yan-Tsung Peng, Keming Cao, and Pamela C. Cosman. Generalization of the dark channel prior for  
615 single image restoration. *IEEE Transactions on Image Processing*, 27(6):2856–2868, 2018.
- 616 Joseph Redmon and Ali Farhadi. Yolov3: An incremental improvement. *arXiv*, 2018.
- 617 Shaoqing Ren, Kaiming He, Ross B. Girshick, and Jian Sun. Faster R-CNN: towards real-time  
618 object detection with region proposal networks. *TPAMI*, 39(6):1137–1149, 2017.
- 619 Tarun Sharma, Danelle E. Cline, and Duane Edgington. Making use of unlabeled data: Compar-  
620 ing strategies for marine animal detection in long-tailed datasets using self-supervised and semi-  
621 supervised pre-training. In *Proceedings of the IEEE/CVF Conference on Computer Vision and  
622 Pattern Recognition (CVPR) Workshops*, pp. 1224–1233, June 2024.
- 623 Tahira Shehzadi, Khurram Azeem Hashmi, Didier Stricker, and Muhammad Zeshan Afzal. Sparse  
624 semi-detr: Sparse learnable queries for semi-supervised object detection. In *Proceedings of the  
625 IEEE/CVF Conference on Computer Vision and Pattern Recognition (CVPR)*, pp. 5840–5850,  
626 June 2024.
- 627 Zhi Tian, Chunhua Shen, Hao Chen, and Tong He. FCOS: fully convolutional one-stage object  
628 detection. In *ICCV*, 2019.
- 629 Xinjiang Wang, Xingyi Yang, Shilong Zhang, Yijiang Li, Litong Feng, Shijie Fang, Chengqi Lyu,  
630 Kai Chen, and Wayne Zhang. Consistent-teacher: Towards reducing inconsistent pseudo-targets  
631 in semi-supervised object detection. In *Proceedings of the IEEE/CVF Conference on Computer  
632 Vision and Pattern Recognition (CVPR)*, pp. 3240–3249, June 2023a.
- 633 Yi Wang, Hui Liu, and Lap-Pui Chau. Single underwater image restoration using adaptive  
634 attenuation-curve prior. *IEEE Transactions on Circuits and Systems I: Regular Papers*, 65(3):  
635 992–1002, 2018.
- 636 Zhenyu Wang, Ya-Li Li, Ye Guo, and Shengjin Wang. Combating noise: Semi-supervised learning  
637 by region uncertainty quantification. In M. Ranzato, A. Beygelzimer, Y. Dauphin, P.S. Liang, and  
638 J. Wortman Vaughan (eds.), *Advances in Neural Information Processing Systems*, volume 34, pp.  
639 9534–9545. Curran Associates, Inc., 2021.
- 640 Zhizhong Wang, Lei Zhao, and Wei Xing. Stylediffusion: Controllable disentangled style transfer  
641 via diffusion models. In *Proceedings of the IEEE/CVF International Conference on Computer  
642 Vision (ICCV)*, pp. 7677–7689, October 2023b.

648 Mengde Xu, Zheng Zhang, Han Hu, Jianfeng Wang, Lijuan Wang, Fangyun Wei, Xiang Bai, and  
649 Zicheng Liu. End-to-end semi-supervised object detection with soft teacher. In *2021 IEEE/CVF*  
650 *International Conference on Computer Vision (ICCV)*, pp. 3040–3049, 2021.

651 Dehuan Zhang, Jingchun Zhou, Weishi Zhang, ChunLe Guo, and Chongyi Li. Synergistic multiscale  
652 detail refinement via intrinsic supervision for underwater image enhancement. *arXiv preprint*  
653 *arXiv:2308.11932*, 2023a.

654 Dehuan Zhang, Jingchun Zhou, Chunle Guo, Weishi Zhang, and Chongyi Li. Synergistic multiscale  
655 detail refinement via intrinsic supervision for underwater image enhancement. *Proceedings of the*  
656 *AAAI Conference on Artificial Intelligence*, 38(7):7033–7041, Mar. 2024.

657 Jiacheng Zhang, Xiangru Lin, Wei Zhang, Kuo Wang, Xiao Tan, Junyu Han, Errui Ding, Jingdong  
658 Wang, and Guanbin Li. Semi-detr: Semi-supervised object detection with detection transformers.  
659 In *2023 IEEE/CVF Conference on Computer Vision and Pattern Recognition (CVPR)*, pp. 23809–  
660 23818, 2023b.

661 Weidong Zhang, Peixian Zhuang, Hai-Han Sun, Guohou Li, Sam Kwong, and Chongyi Li. Un-  
662 derwater image enhancement via minimal color loss and locally adaptive contrast enhancement.  
663 *IEEE Transactions on Image Processing*, 31:3997–4010, 2022.

664 Hongyu Zhou, Zheng Ge, Songtao Liu, Weixin Mao, Zeming Li, Haiyan Yu, and Jian Sun. Dense  
665 teacher: Dense pseudo-labels for semi-supervised object detection. In Shai Avidan, Gabriel Bros-  
666 tow, Moustapha Cissé, Giovanni Maria Farinella, and Tal Hassner (eds.), *Computer Vision –*  
667 *ECCV 2022*, pp. 35–50, Cham, 2022. Springer Nature Switzerland.

668  
669  
670  
671  
672  
673  
674  
675  
676  
677  
678  
679  
680  
681  
682  
683  
684  
685  
686  
687  
688  
689  
690  
691  
692  
693  
694  
695  
696  
697  
698  
699  
700  
701